Electrochimica Acta 54 (2009) 3872–3876

Contents lists available at ScienceDirect

Electrochimica Acta

journal homepage: www.elsevier.com/locate/electacta

Promising Ni–Fe–LSGMC anode compatible with lanthanum gallate electrolyte

Shizhong Wang[a,b,*], Qiong He[a], Meilin Liu[b,**]

[a] Department of Chemistry, College of Chemistry and Chemical Engineering, Xiamen University, Xiamen, Fujian 361005, PR China
[b] School of Materials Science and Engineering, Georgia Institute of Technology, Atlanta, GA 30332-0245, USA

ARTICLE INFO

Article history:
Received 29 November 2008
Received in revised form 29 January 2009
Accepted 1 February 2009
Available online 10 February 2009

Keywords:
Lanthanum gallate
Anode
Iron
Nickel
Compatibility

ABSTRACT

A number of composite materials in the Ni–Fe–LSGMC family have been studied as potential anodes for solid oxide fuel cells (SOFCs) based on strontium, magnesium, and cobalt doped lanthanum gallate electrolyte (LSGMC). The results show that Ni reacts with LSGMC especially under reducing conditions at high temperatures, resulting in high contact resistance, large electrode polarization, and poor performance. The reaction between Ni and LSGMC depends strongly on the composition and pre-sintering temperature of LSGMC, the concentration of iron in the electrode, and the processing and operating temperatures. Under proper conditions, Ni–Fe–LSGMC5 could be a promising high-performance anode with good compatibility with LSGMC5 electrolyte.

1. Introduction

Solid oxide fuel cells (SOFCs) have attracted much attention due to their high-energy efficiency, potential long-term stability, and excellent fuel flexibility – the potential for direct utilization of hydrocarbon fuels, coal gas, biomass, and other renewable fuels. However, SOFCs must be economically competitive to be commercially viable. Significant efforts are being made to lower the operating temperature of SOFCs in order to further reduce the cost and improve the reliability and operational life. Lowering the operating temperature will allow the use of less expensive materials for cell components; unfortunately, it also lowers the fuel cell performance, as the electrolyte materials become less conductive and the electrodes less catalytically active. Thus, the development of highly efficient electrode and highly conductive electrolyte materials is vital to the success in the development of cost-effective intermediate- or low-temperature SOFCs.

Doped lanthanum gallate is a promising electrolyte for intermediate temperature SOFCs due to its high oxygen ion conductivity, negligible electronic conductivity, and high chemical stability at intermediate temperatures over a wide range of oxygen partial pressures [1]. There are growing interests in developing high-performance electrodes for SOFCs based on lanthanum gallate [2].

A metal–ceramic composite consisting of Ni and doped ceria has been reported to be a promising anode for SOFCs based on lanthanum gallate electrolyte [3]. The addition of an ionically conducting ceramic phase (e.g., doped ceria) improves the microstructural stability and catalytic activity of Ni by extending the length of the triple-phase boundaries (TPB). Lanthanum gallate itself would be a promising ceramic phase for the composite electrodes since Ni-YSZ and LSM-YSZ are the most widely used anode and cathode for SOFCs based on YSZ electrolyte. Indeed, cobalt, strontium, and magnesium doped lanthanum gallate (LSGMC) have been successfully used to improve the stability and activity of $Sm_{0.5}Sr_{0.5}CoO_3$ (SSC) cathodes supported on lanthanum gallate [4]. For the anodes, unfortunately, significant reaction between Ni and LSGMC8.5 ($La_{0.8}Sr_{0.2}Ga_{0.8}Mg_{0.115}Co_{0.085}O_3$) was observed [5] although a composite consisting of Ni–Fe–LSGMC8.5 showed high performance for the oxidation of H_2 and di-methyl ether. Zhang et al. [6] also found that NiO reacts with lanthanum gallate during the sintering process, resulting in a dramatic decrease in electrical conductivity and electrode performance [7].

On the other hand, He et al. [8] found that the addition of Cu into the composite of Ni and lanthanum gallate significantly impedes the reaction between Ni and lanthanum gallate. However, the activity of the electrode was rather low due to the poor catalytic activity of Cu. Thus, other additives are needed to improve not only the compatibility between Ni and lanthanum gallate but also the performance of the composite anode.

In this paper, we report our findings in investigations into the stability and the catalytic activity of a series of Ni–Fe–LSGMC composite anodes using XRD, SEM, and impedance spectroscopy.

* Corresponding author. Present address: GE (China) Research and Development Center Co. Ltd., 1800 Cailun Road, Pudong, Shanghai 201203, China.
** Corresponding author.
E-mail addresses: shizwang@sohu.com (S. Wang), meilin.liu@mse.gatech.edu (M. Liu).

0013-4686/$ – see front matter © 2009 Elsevier Ltd. All rights reserved.
doi:10.1016/j.electacta.2009.02.002

2. Experimental

The precursors used for electrolytes $La_{0.8}Sr_{0.2}Ga_{0.8}Mg_{0.15}Co_{0.05}O_3$ (LSGMC5) and $La_{0.8}Sr_{0.2}Ga_{0.8}Mg_{0.115}Co_{0.085}O_3$ (LSGMC8.5) were La_2O_3 (99.99%), $SrCO_3$ (99.99%), MgO (99.99%), Ga_2O_3 (99.99%) and CoO (99.9%), all from Sigma–Aldrich. Powders of these precursors were mixed in stoichiometric ratio using a mortar and pestle for 30 min and then calcined at 1273 K for 6 h. The resulting product was iso-statically pressed into a disk at 274.6 MPa for 10 min. The diameter of the green pellets was ~2.0 cm. The disks were then sintered at 1773 K for 6 h in air. The sintered disks were ground and polished to a thickness of 0.3 mm.

The composite anode Ni–Fe–LSGMC5 and Ni–Fe–LSGMC8.5 were prepared as follows. The precursors for LSGMC8.5 and LSGMC5 were calcined at 1273–1573 K for 6 h after grinding and pre-firing at 1273 K for 2 h. Unless stated otherwise, all composite anodes and the electrolyte powders were fired at 1473 K. $Ni(NO_3)_2{\cdot}6H_2O$ (99%), Fe_2O_3(99.9%), and LSGMC8.5 or LSGMC5 in stoichiometric ratio were then added into a beaker containing suitable amount of water. After boiling and drying under vigorous stirring, the residue was fired at 1273 K for 2 h. Composite anodes with a molar ratio of Ni to Fe about 10/0, 9/1, 8/2, 7/3, 6/4 and 5/5 were prepared. The weight percentage of LSGMC8.5 or LSGMC5 in the composite electrode was 25%. The electrodes were denoted as Ni_{10}–Fe_0–LSGMC8.5, in which the ratio of Ni to Fe and the type of the electrolyte powder were shown clearly.

$Sm_{0.5}Sr_{0.5}CoO_3$(SSC)–LSGMC5 composite cathodes were also prepared using a solid-state reaction method as reported elsewhere [5].

The test cells with configuration of anode/electrolyte/cathode were fabricated as follows. First, anode paste was screen-printed on an electrolyte pellet and fired at 1473 K for 2 h. SSC–LSGMC5 composite cathode was then screen-printed on the other side of the electrolyte symmetrically [9]. A Pt reference electrode was prepared on the cathode side. The cathode and reference electrode were then fired at 1223 K for 0.5 h. The effective electrode areas for both the anode and cathode were 0.2 cm^2. Pt meshes were used to cover the surface of the anode and cathode, respectively, as the current collector. Pt lead wires were used to connect the electrodes to electrochemical equipments. 100 ml min^{-1} H_2 saturated with 298 K water was supplied as the fuel, and 100 ml min^{-1} pure oxygen was used as the oxidant.

All electrochemical measurements were performed using a VMP2/Z-40(AMETECH) electrochemical testing station. The frequency range for the impedance measurements was usually 0.01 Hz–100 kHz, and the amplitude of the input sinuous signal was 10 mV. The phase composition of the materials was identified using XRD (Panalytical X'pert). For XRD characterizations, all electrodes were fired at 1473 K for 2 h in air followed by reduction in H_2 for 1 h at different temperatures. The morphology of the electrodes after electrochemical testing was examined using scanning electron microscopy (XL30 ESEM).

3. Results and discussion

3.1. Phase composition

Shown in Fig. 1(a) and (b) are the original and enlarged XRD patterns of several Ni–Fe–LSGMC8.5 electrodes, respectively, with different ratios of Fe to Ni, fired at 1473 K in air for 2 h. Phases corresponding to $La_{0.8}Sr_{0.2}Ga_{0.85}Mg_{0.15}O_{2.825}$, $Ni_{1.25}Fe_{1.85}O_4$, and NiO can be clearly identified in Fig. 1(a). With the increase in the ratio of Fe to Ni, the intensities of the peaks corresponding to NiO decreased, while those corresponding to $Ni_{1.25}Fe_{1.85}O_4$ increased. In the enlarged part shown in Fig. 1(b), a small peak corresponding to $SrLaGa_3O_7$ can be observed, suggesting a reaction between NiO and

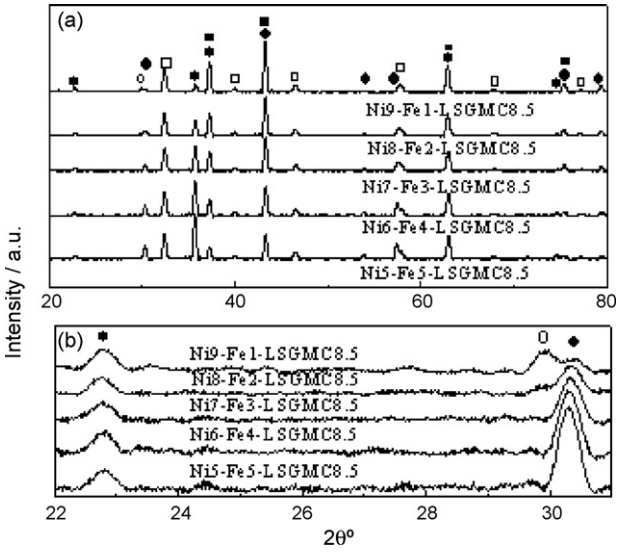

Fig. 1. XRD patterns of various Ni–Fe–LSGMC8.5 composite anodes sintered at 1473 K in air for 2 h (a), and enlarged figure of selected part (b). ●, $Ni_{1.25}Fe_{1.85}O_4$ (01-088-0380); ■, NiO (01-075-0197); ○, $SrLaGa_3O_7$ (01-086-1839); □, $La_{0.8}Sr_{0.2}Ga_{0.85}Mg_{0.15}O_{2.825}$ (01-089-4448). The number in the parentheses is the JCPDS card number.

lanthanum gallate [7]. The intensity of $SrLaGa_3O_7$ peak decreases with increasing concentration of Fe in the electrode, and clear peak only appears in Ni_9–Fe_1–LSGMC8.5.

XRD patterns of Ni–Fe–LSGMC8.5 changed dramatically after reduction in hydrogen at 1248 K for 1 h. As reported previously [5], XRD patterns resembling that of Ni were observed, which shifted to lower 2θ values with the increase in the concentration of Fe in the electrode. This suggests that Fe dissolved in Ni to form Ni–Fe solid solution. In addition, small peaks corresponding to $SrLaGa_3O_7$ and $La_2NiO_{4.14}$ are also identifiable from the XRD patterns of the reduced Ni–Fe–LSGMC8.5 anodes shown in Fig. 2. The peak intensities of $SrLaGa_3O_7$ and $La_2NiO_{4.14}$ in reduced state electrode shown in Fig. 2 are much higher than those in oxidation state electrode shown in Fig. 1. It is clear that the dominant process for the generation of $SrLaGa_3O_7$ and $La_2NiO_{4.14}$ in the anode is the reaction between LSGMC and Ni metal. With the increase in the ratio of Ni to Fe, the intensities of the peaks corresponding to $SrLaGa_3O_7$ and $La_2NiO_{4.14}$ increased. The peak corresponding to $SrLaGa_3O_7$

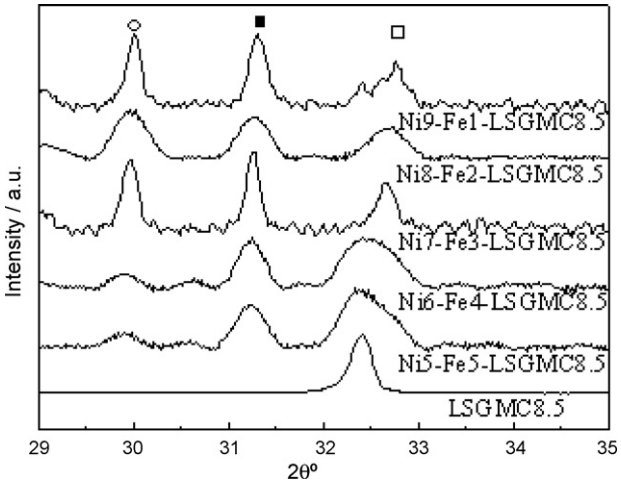

Fig. 2. XRD patterns of various Ni–Fe–LSGMC8.5 composite anodes reduced in H_2 at 1248 K. ■, $La_2NiO_{4.18}$ (01-079-095); ○, $SrLaGa_3O_7$ (01-086-1839); □, $La_{0.8}Sr_{0.2}Ga_{0.85}Mg_{0.15}O_{2.825}$ (01-089-4448). The number in the parentheses is the JCPDS card number.

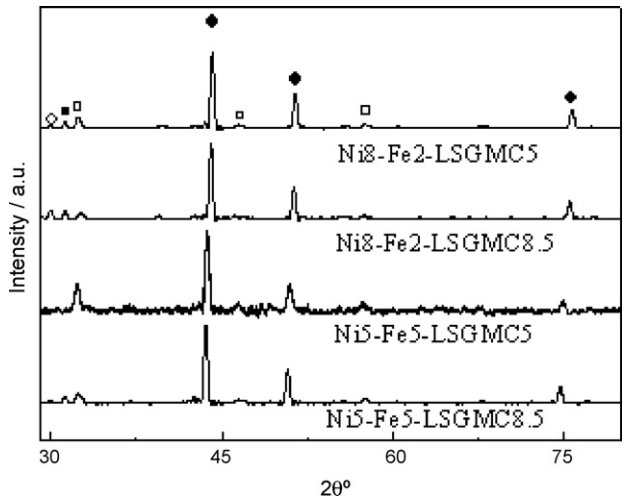

Fig. 3. XRD patterns of various Ni–Fe–LSGMC anodes reduced in H_2 at 1248 K. ●, Ni_3Fe (01-088-1715); ■, $La_2NiO_{4.18}$ (01-079-0951); □, $La_{0.8}Sr_{0.2}Ga_{0.85}Mg_{0.15}O_{2.825}$ (01-089-4448); ○, $SrLaGa_3O_7$ (01-086-1839). The number in the parentheses is the JCPDS card number.

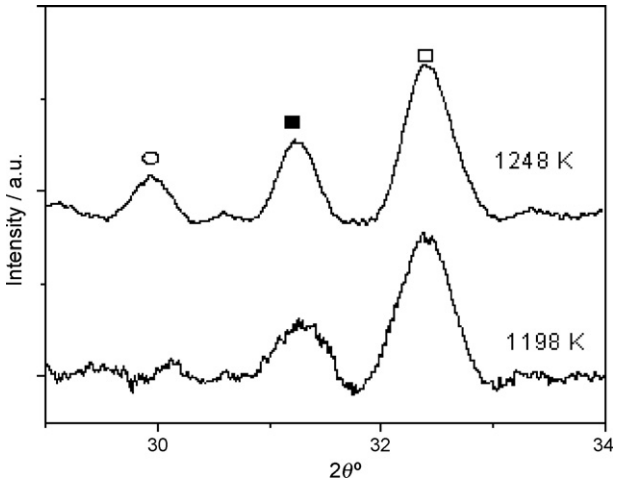

Fig. 4. XRD patterns of Ni_8–Fe_2–LSGMC5 composite anodes reduced at different temperatures. ■, $La_2NiO_{4.18}$ (01-079-095); ○, $SrLaGa_3O_7$ (01-086-1839); □, $La_{0.8}Sr_{0.2}Ga_{0.85}Mg_{0.15}O_{2.825}$ (01-089-4448). The number in the parentheses is the JCPDS card number.

depends more strongly on the concentration of iron in the electrode than that of $La_2NiO_{4.14}$. Another observation is that, with the increase in the ratio of Ni to Fe, the position of the peaks corresponding to LSGMC8.5 shifts to higher 2θ values while the intensities of the peaks are reduced. Fig. 2 suggests that Ni reacts with LSGMC8.5 under reducing conditions at 1248 K, but Fe is effective in extenuating the reaction. Thus, the addition of Fe can effectively improve the chemical compatibility between Ni and lanthanum gallate, making it possible to develop Ni–LSGM composite anodes for SOFCs based on lanthanum gallate electrolyte.

Shown in Fig. 3 are the XRD patterns of Ni_8–Fe_2–LSGMC5 and Ni_5–Fe_5–LSGMC5 electrodes reduced at 1248 K in H_2 for 1 h. As a comparison, the XRD patterns of Ni_8–Fe_2–LSGMC8.5 and Ni_5–Fe_5–LSGMC8.5 electrodes are shown in the same figure. Intense peaks corresponding to phases of Ni–Fe alloys are readily observed in Fig. 3, with a XRD pattern resembling that of Ni_3Fe [5]. The intensities of $SrLaGa_3O_7$ and $La_2NiO_{4.14}$ phase in Ni–Fe–LSGMC5 anodes are much lower than corresponding electrodes containing LSGMC8.5. Further, the intensities of $SrLaGa_3O_7$ and $La_2NiO_{4.14}$ in Ni_5–Fe_5–LSGMC5 and Ni_5–Fe_5–LSGMC8.5 are much lower than corresponding electrodes containing Ni_8–Fe_2. No obvious $SrLaGa_3O_7$ and $La_2NiO_{4.14}$ phases can be identified in the XRD pattern for Ni_5–Fe_5–LSGMC5. It is clear that the reaction between Ni and lanthanum gallate depends strongly on the ratio of Ni to Fe and the composition of the lanthanum gallate powder used in the electrode, especially the concentration of cobalt in the electrolyte powder. Lanthanum gallate containing low concentration of cobalt seems to have good chemical compatibility with Ni.

Shown in Fig. 4 are the XRD patterns of Ni_8–Fe_2–LSGMC5 reduced in H_2 at 1198 and 1248 K for 1 h, respectively. The peak corresponding to $SrLaGa_3O_7$ becomes smaller as the reduction temperature was lowered, and no obvious $SrLaGa_3O_7$ phase can be identified in the anode reduced at 1198 K. The ratio of the intensity of $La_2NiO_{4.14}$ to LSGMC5 also decreases from 0.4 to 0.3 with the decrease in reduction temperature from 1248 to 1198 K. It is clear that the formation of $SrLaGa_3O_7$ and $La_2NiO_{4.14}$ depends strongly on reduction temperature. The reaction between Ni and LSGMC5 would be negligible when the operation temperature of fuel cells is much lower than 1198 K.

Shown in Fig. 5 are the XRD patterns of Ni_8–Fe_2–LSGMC5 calcined in air consisted of LSGMC5 fired at various temperatures. Similar to the cases of Ni–Fe–LSGMC8.5, phases corresponding to $La_{0.8}Sr_{0.2}Ga_{0.85}Mg_{0.15}O_{2.825}$, $Ni_{1.25}Fe_{1.85}O_4$, and NiO can be observed, but no new obvious phases can be identified. After reduction in H_2 at 1198 K, new peak corresponding to $La_2NiO_{4.14}$ appears besides those of $La_{0.8}Sr_{0.2}Ga_{0.85}Mg_{0.15}O_{2.825}$ and Ni–Fe alloys as shown in Fig. 6. The peak corresponding to $La_2NiO_{4.14}$ becomes smaller with the increase in the calcination temperatures for the LSGMC5 powder; the ratio of the peak for $La_2NiO_{4.14}$ to that for Ni–Fe alloy are 0.12, 0.10, 0.09, and 0.06 for the anodes containing LGMC5 fired at 1273, 1373, 1473 and 1573 K, respectively. It is clear that the chemical compatibility between Ni and LSGMC5 depends strongly on the calcination temperature of the LSGMC5 powder. Higher firing temperature of LGMC5 effectively diminishes the reactivity between Ni and LSGMC5.

3.2. Microstructures of Ni–Fe–LSGMC5 anodes

Shown in Fig. 7 are the cross-sectional views (SEM images) of some typical Ni–Fe–LSGMC5 anodes with different ratios of Ni to Fe. It can be seen that the morphology of the electrode and electrode/electrolyte interface are closely related to the ratio of Ni to Fe

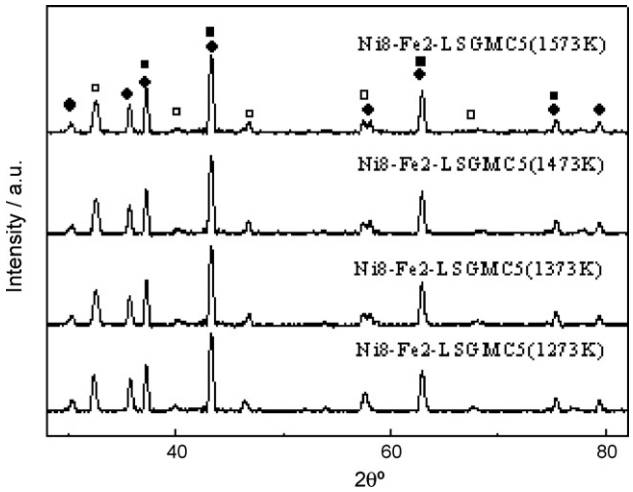

Fig. 5. XRD patterns of Ni_8–Fe_2–LSGMC5 composite anodes calcined in air consisted of LSGMC5 powder sintered at different temperatures. ●, $Ni_{1.25}Fe_{1.85}O_4$ (01-088-0380); ■, NiO (01-075-0197); □, $La_{0.8}Sr_{0.2}Ga_{0.85}Mg_{0.15}O_{2.825}$ (01-089-4448). The number in the parentheses is the JCPDS card number.

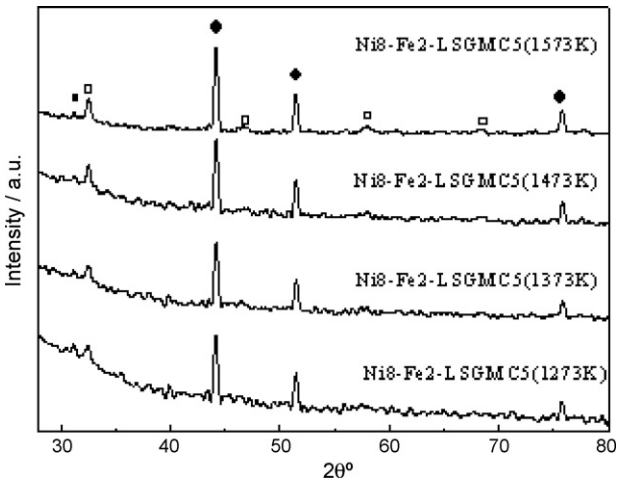

Fig. 6. XRD patterns of Ni_8–Fe_2–LSGMC5 composite anodes reduced in H_2 at 1198 K consisted of LSGMC5 powders sintered at different temperatures. ●, Ni_3Fe (01-088-1715); ■, $La_2NiO_{4.18}$ (01-079-0951); □, $La_{0.8}Sr_{0.2}Ga_{0.85}Mg_{0.15}O_{2.825}$ (01-089-4448). The number in the parentheses is the JCPDS card number.

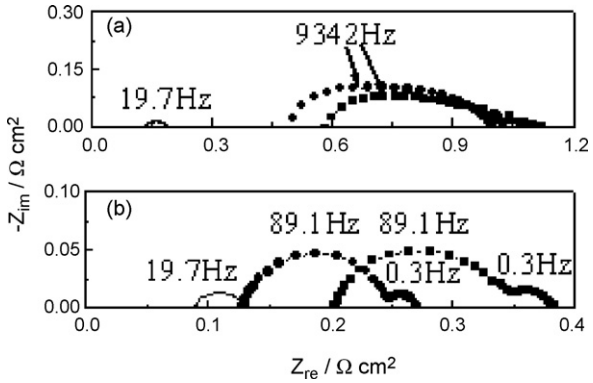

Fig. 8. Impedance spectra of cells with (a) Ni_{10}–Fe_0–LSGMC5 anode and (b) Ni_8–Fe_2–LSGMC5 anode measured at 1073 K under open circuit conditions using a two-electrode and three-electrode configuration: ■, full cell; ●, anode side; —, cathode side. The number appearing in the figure is the frequency of the summit of the spectrum.

in the electrode. With the increase in the molar ratio of Fe to Ni, the size of the electrode grains increased, the porosity decreased, and the adhesion of the anode to the electrolyte was visibly improved, leading to an increase in the electrode/electrolyte two-phase contact area. Since Ni–Fe–LSGMC5 is a composite mixed-conducting electrode, both the change in TPB length and two-phase contact area may influence the electrochemical performance. However, the ideal morphology and microstructure for thus a composite electrode is still an open question since the charge and mass transfer processes involved in anode reactions are very complex, including transport of fuel molecules to (and reaction products away from) the active sites for fuel oxidation through the pores or along the pore surfaces, charge transfer across the interfaces or electrode surfaces, as well as the ionic and electronic current flow through the solid phase.

3.3. Electrochemical characterization

Shown in Fig. 8 are the impedance spectra of the anode, the cathode, and the full cell at 1073 K under open circuit conditions for button cells with an anode of (a) Ni_{10}–Fe_0–LSGMC5 and (b) Ni_8–Fe_2–LSGMC5. A two-electrode configuration was used to determine the impedance of the entire cell, from which the ohmic resistance of the cell can be separated from the electrode polarization resistance. To determine the anode and the cathode impedance separately, a three-electrode configuration was used. For each spectrum, the intercept of the impedance arc at high frequencies represents the ohmic resistance while the diameter of the impedance loop corresponds to the electrode polarization resistance.

It can be seen from Fig. 8(a) the impedances acquired from the cathode side are much smaller than those from the anode side or from the full cell. Both ohmic resistance and electrode polarization resistance of the anode are much greater than those of the cathode; in fact, they are close to those of the full cell. It is clear that the cathode is much more active than the anode for the cell based on Ni_{10}–Fe_0–LSGMC5 anode and SSC–LSGMC5 cathode. The impedances of the anode side for the cell with a Ni_8–Fe_2–LSGMC5 anode, shown in Fig. 8(b), are smaller than those for the cell with Ni_{10}–Fe_0–LSGMC5, shown in Fig. 8(a). The ohmic resistances of the cathode side shown in Fig. 8(a) and (b) are 0.13 and 0.09 $\Omega\,cm^2$, respectively, whereas the polarization resistances of the cathode side shown in Fig. 8(a) and (b) are 0.059 and 0.044 $\Omega\,cm^2$, respectively. While the cathode resistances for the two cells are different, the errors are relatively small compared with the impedances of the anodes.

The difference in ohmic resistances between the two full cells, shown in Fig. 8(a) and (b), is about 0.37 $\Omega\,cm^2$, which is very close to the difference in ohmic resistance between the two impedance spectra from the anode side of the two cells, 0.36 $\Omega\,cm^2$. Further, the difference in electrode polarization resistances between

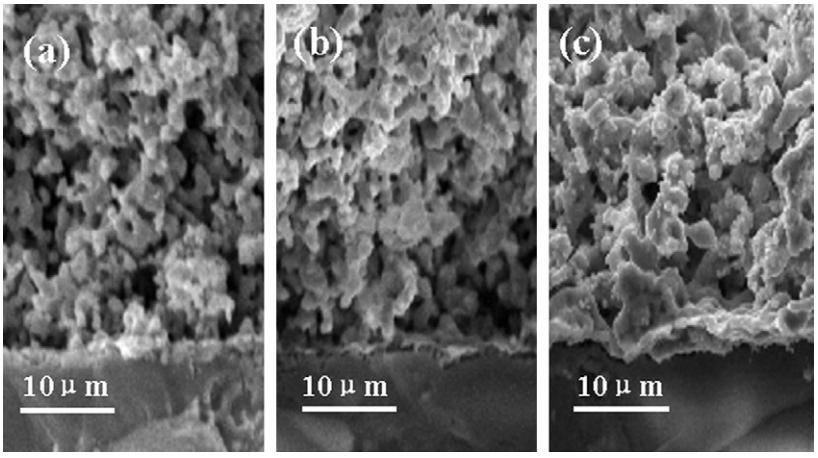

Fig. 7. SEM images of the cross-section of various Ni–Fe–LSGMC5 composite anodes: (a) Ni_{10}–Fe_0-LSGMC5, (b) Ni_8–Fe_2–LSGMC5, and (c) Ni_5–Fe_5–LSGMC5.

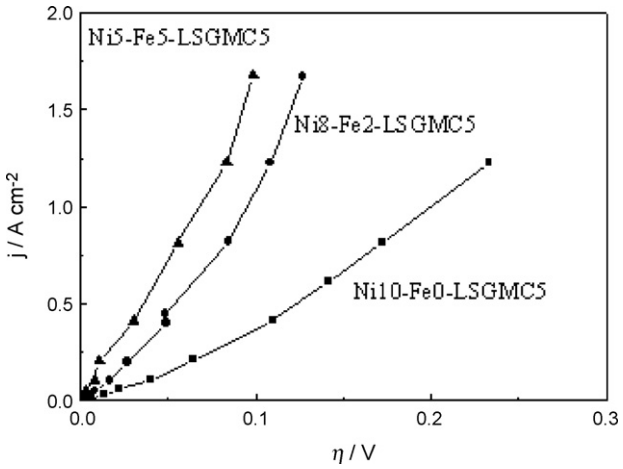

Fig. 9. Anodic polarization curves of various Ni–Fe–LSGMC5 anodes at 1073 K.

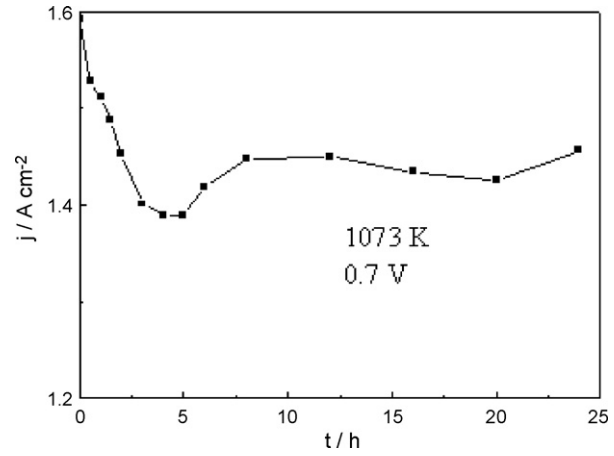

Fig. 10. Current density as a function of time at 1073 K under a terminal voltage of 0.7 V of a Ni_8–Fe_2–LSGMC5/LSGMC5/SSC-LSGMC5 cell.

the two full cells is about 0.37 Ω cm^2, which is also very close to the 0.39 Ω cm^2, the difference in anode polarization resistances of the two cells. These results suggest that the cell with a Ni_{10}–Fe_0–LSGMC5 anode has a much higher ohmic resistance and anode polarization resistance than that with a Ni_5–Fe_5–LSGMC5 anode. One explanation is that the reactions between Ni and LSGMC5 in the absence of Fe produce more resistive phases such as $SrLaGa_3O_7$ [6–7] as evident from the XRD analysis. The increase in the ratio of Fe to Ni impedes the reaction between Ni and lanthanum gallate, leading to a decrease in ohmic resistance and polarization resistance.

Other effects are related to the differences in morphology, microstructure, and the catalytic activity of Ni, Fe, and Fe–Ni alloys in the anodes. As shown in Fig. 7, the electrode/electrolyte two-phase contact area increased with the ratio of Fe to Ni, improving the bonding between the two phases and current flow across the interface [10]. Further, Fe adsorbs oxygen strongly [11], which would also influence the activity of the composite anode for hydrogen oxidation [12]. It was also reported that Ni_3Fe phase possesses higher catalytic ability for dissociation of H_2 [13] and lower hydrogen desorption energy [14] compared with Ni. Therefore, the high catalytic activity of Fe and/or Ni_3Fe phase could also be one of the reasons for the observed high activity of the Ni–Fe composite anodes [15].

Shown in Fig. 9 are the anodic polarization curves of Ni_{10}–Fe_0–LSGMC5, Ni_8–Fe_2–LSGMC5 and Ni_5–Fe_5–LSGMC5 at 1073 K. The overpotentials of these electrodes are in the order of Ni_{10}–Fe_0–LSGMC5 > Ni_8–Fe_2–LSGMC5 > Ni_5–Fe_5–LSGMC5 at a given current density. Again, the activity of the electrode increased with the ratio of Fe to Ni in the electrode, consistent with the impedance measurements shown in Fig. 8.

Shown in Fig. 10 is the stability of a cell with a Ni_8–Fe_2–LSGMC5 anode tested at a constant 0.7 V cell voltage at 1073 K for a short period of time. The current of the cell decreased slightly in the first 2–3 h, and then recovered and remained stable up to 24 h, suggesting that Ni–Fe–LSGMC5 could be a potential stable electrode with high performance and good compatibility with LSGMC5 electrolyte.

4. Conclusions

Ni reacts with $La_{0.8}Sr_{0.2}Ga_{0.8}Mg_{0.115}Co_{0.085}O_3$ (LSGMC8.5) under reducing conditions at high temperatures, resulting in increased ohmic resistance and high electrode polarization resistance. The addition of iron is effective in improving the chemical compatibility between Ni and lanthanum gallate. In particular, we demonstrated that $La_{0.8}Sr_{0.2}Ga_{0.8}Mg_{0.15}Co_{0.05}O_3$ (LSGMC5) had a much higher compatibility with Ni than LSGMC8.5. Further, a cell with a Ni–Fe–LSGMC5 anode showed promising preliminary performance, suggesting that it could be a promising anode with adequate compatibility with LSGMC5 electrolyte.

Acknowledgements

This material is based upon work supported by the "Fujian Province Science and Technology Program, Key Project (No. 2003H046)" and Research Fund for Homecoming scholars.

References

[1] T. Ishihara, H. Matsuda, Y. Takita, J. Am. Chem. Soc. 116 (1994) 3801.
[2] Y. Hiei, T. Ishihara, Y. Takita, Solid State Ionics 86–88 (1996) 1267.
[3] S. Wang, T. Ishihara, Y. Takita, Electrochem. Solid State Lett. 5 (8) (2002) A177.
[4] S. Wang, Y. Zou, Electrochem. Commun. 8 (2006) 927.
[5] S. Wang, J. Gao, Electrochem. Solid State Lett. 9 (9) (2006) A395.
[6] X. Zhang, S. Ohara, H. Okawa, R. Maric, T. Fukui, Solid State Ionics 139 (2001) 145.
[7] X. Zhang, S. Ohara, R. Maric, K. Mukai, T. Fukui, H. Yoshida, M. Nishimura, T. Inagaki, K. Miura, J. Power Sources 83 (1999) 170.
[8] T. He, P. Guan, L. Cong, Y. Ji, H. Sun, J. Wang, J. Liu, J. Alloys Compd. 393 (2005) 292.
[9] T. Kato, A. Momma, Y. Kaga, S. Nagata, Y. Kasuga, M. Kitase, Solid State Ionics, 132 3–4 (2002) 287.
[10] J. Fleig, J. Maier, J. Electrochem. Soc. 144 (11) (1997) L302.
[11] T. Horita, N. Sakai, T. Kawada, H. Yokokawa, M. Dokiya, J. Electrochem. Soc. 143 (4) (1996) 1161.
[12] S. Primdahl, M. Mogensen, J. Electrochem. Soc. 144 (10) (1997) 3409.
[13] X. Zhong, J. Zhu, A.H. Zhang, Intermetallics 15 (2007) 495.
[14] J. Wang, W.J. Chia, Y.W. Chung, C.T. Liu, Intermetallics 8 (2000) 353.
[15] X.C. Lu, J.H. Zhu, J. Power Sources 165 (2007) 678.